NASA Technical Memorandum 102050

Arcjet Nozzle Design Impacts

Francis M. Curran
Lewis Research Center
Cleveland, Ohio

Amy J. Sovie
Ohio University
Athens, Ohio

and

Thomas W. Haag
Lewis Research Center
Cleveland, Ohio

Prepared for the
1989 JANNAF Propulsion Meeting
Cleveland, Ohio, May 23-25, 1989

NASA

ARCJET NOZZLE DESIGN IMPACTS

Francis M. Curran
National Aeronautics and Space Administration
Lewis Research Center
Cleveland, Ohio 44135

Amy J. Sovie*
Ohio University
Electrical Engineering Department
Athens, Ohio 45701

and

Thomas W. Haag
National Aeronautics and Space Administration
Lewis Research Center
Cleveland, Ohio 44135

E-4802

ABSTRACT

An experimental investigation was conducted to determine the effect of nozzle configuration on the operating characteristics of a low power dc arcjet thruster. A conical nozzle with a 30° converging angle, a 20° diverging angle, and an area ratio of 225 served as the baseline case for the study. Variations on the geometry included bell-shaped contours both up and downstream, and a downstream trumpet-shaped contour. The nozzles were operated over a range of specific power near that anticipated for on-orbit operation. Mass flow rate, thrust, current, and voltage were monitored to provide accurate comparisons between nozzles. The upstream contour was found to have minimal effect on arcjet operation. It was determined that the contour of the divergent section of the nozzle, that serves as the anode, was very important in determining the location of arc attachment, and thus had a significant impact on arcjet performance. The conical nozzle was judged to have the optimal current/voltage characteristics and produced the best performance of the nozzles tested.

INTRODUCTION

Low powered dc arcjet thrusters were first proposed for space propulsion in the mid-1950's and a subsequent NASA-sponsored research and development program continued into the early 1960's. This effort culminated in the successful, uninterrupted lifetesting of a 2 kW hydrogen arcjet at the Plasmadyne Corporation[1] and in the manufacture of a 1 kW hydrogen arcjet flight system designed for the Space Electric Rocket Test (SERT) program.[2,3] This unit was never flown and ground test results indicated unacceptable electrode erosion. Propellants other than hydrogen were tried with the 1 kW engine with similar results. A review of the early arcjet program that includes test results of the 1 and 2 kW thrusters was published by Wallner and Czika in 1965.[4] After the early 1960's, interest in arcjets waned and there was no serious development for the next 20 years.

In recent years, the need for increased spacecraft life has driven a reevaluation of the practicality of arcjets for missions such as north-south stationkeeping (NSSK) on geosynchronous communications satellites. The use of arcjets is particularly timely given the projections of increased electrical power available for use in propulsion (3 to 5 kW) on 1990's satellites. The ongoing NASA-sponsored research program, restarted in 1983, has demonstrated stable, nondestructive operation of low power (1 to 2 kW) arcjet thrusters on storable propellants, or mixtures simulating their decomposition products, over a wide range of mass flow rate.[5-13] Performance data from this work have indicated that specific impulse values of more than 450 sec can be expected for power and mass flow rates typical of NSSK mission scenarios.[14,15] In addition, a long term, cyclic, automated arcjet lifetest to demonstrate reliability[16] has been performed and the effects of both plume impacts[17,18] and electromagnetic interference (EMI) are under investigation.

While the current test program indicates that the low power arcjet is nearing flight readiness, basic research aimed at improving the overall operating characteristics also continues. One goal of this research is the optimization of nozzle configuration. In the past, many analytical and experimental studies have been undertaken in an attempt to gain better understanding of nozzle effects on flows characterized by low Reynolds numbers (Re) typical of arcjet thrusters (<1000) (see, for example, Refs. 19 to 26). Early work by Spisz, et al.,[19] examined heated hydrogen flow in conical (20° divergence angle) nozzles with varying area ratios. The results showed that at Re of about 500, the thrust coefficient reached a maximum at a low area ratio (~6). A more extensive examination[20] included hydrogen and nitrogen as propellants with variations in nozzle shape, cone angle and

*Summer Student Intern at NASA Lewis Research Center.

area ratio. Here calculations and experiments showed a slight efficiency advantage for a trumpet shape compared to a bell and cone shape. A 20° cone was judged better than cones of 10° and 35°. For a 20° conical nozzle, the smallest area ratio tested (20) gave the best results in agreement with the previous study. In 1971, Rae described an implicit finite differencing scheme for solving the slender channel equations to model low Re flows for small rockets.[21] His results suggested that wide divergence angles and low area ratios should be employed to optimize performance. The results also indicated that small angles could lead to cases in which supersonic flow would not be present (i.e., viscous layer dominated flow). Kallis, et al., used a slightly modified version of Rae's formulation to analyze the performance of biowaste resistojets.[22] In this study, performance predictions compared reasonably with experimental results. In perhaps the most fundamental experimental analysis to date, Rothe studied low Re (100 to 1000) flows in a 20° conical nozzle using electron beam fluorescence techniques.[23] Gas temperature and density measurements indicated fully viscous flow for Re of about 300 and that a supersonic bubble can occur in flows at Re approximately equal to 100. Kuluva and Hosack developed a simple formula for the calculation of nozzle discharge coefficients[24] using a boundary layer analysis. Their analysis suggested that the curvature of the throat is important at Re near 200 and that at Re at and below 50, the viscous layer can fill the entire throat.

Gas dynamic lasers employ nozzles similar to those used for space propulsion. In 1976, Cline developed a code known as VNAP (Viscous Nozzle Analysis Program) to calculate flow in such nozzles.[25] Cline modified an existing inviscid code utilizing the explicit MacCormack numerical scheme to solve the viscous equations. This formulation is widely applied and was recently used as a tool in the optimization of a flight-type arcjet nozzle.[8] Recently, Penko has developed an implicit code to solve the Navier-Stokes equations in conservative form for the analysis of low Re compressible flow.[26] This predicts the supersonic "bubble" phenomena observed by Rothe.[23]

While the studies discussed above have been helpful in understanding nozzle flow phenomena in small resistojet thrusters, they serve only as a starting point for nozzle optimization in arcjet thrusters. Actually, three interdependent phenomena must be included for a complete nozzle analysis. First is the arc energy addition process which both heats the gas in the sub-, trans-, and supersonic regions and causes excitation, ionization, and dissociation. Second, the position and characteristics of the arc attachment zones affect arc stability, length and the overall thermal efficiency of the device, in addition to local electrode heating and erosion. These phenomena are dependent on mass flow rate, total current and geometry. Third, propellant swirl must be considered. Swirl of the flow is introduced to reduce starting transients and to improve steady state operational stability. Early efforts to model the arc heating process in the constrictor of the arcjet were made by a number of authors.[27-30] Later, both Neuberger[31,32] and Schaeffer[33] developed codes to model a constricted arc in a flow field that included weak swirl. None of these models, however, dealt with phenomena occurring anywhere but in the throat region. Very recently, research aimed at modeling the entire low power arcjet flow field began,[34-36] but has not yet produced useful design tools for arcjet analysis.

This report describes the results of an experimental program designed to improve the understanding of nozzle geometry on arcjet operation. In this program, a number of nozzle configurations were tested at power levels between 0.7 and 1.5 kW using a modular arcjet thruster. Hydrogen/nitrogen mixtures were used to simulate the decomposition products of hydrazine at mass flow rates typical of a blowdown system on a communications satellite.

APPARATUS

ARCJET THRUSTER

An arcjet thruster of the conventional constricted arc design was used in each nozzle test. A cross-sectional schematic of this type of thruster with the baseline conical nozzle insert (described in the next section) in place is shown in Fig. 1.

The cathode was made from a 2 percent thoriated tungsten rod 3.2 mm in diameter and approximately 190 mm in length with the tip initially ground to a 30° half angle. A modified stainless steel compression type gas fitting was used to feed the cathode through the rear insulator, adjust the arc gap, and lock the cathode into position. This, in turn, was held in place by a threaded, center-drilled holding bolt. A graphite foil gasket was inserted between the rear insulator and the fitting to give a gas-tight seal.

The propellant tube entered through the side of the rear insulator through a fitting and threaded into a cylindrical stainless steel anchor. The anchor was center-drilled to allow passage of both the cathode and an insulating alumina sleeve. This arrangement served to isolate the electrodes from the propellant tube.

Each nozzle insert was machined from 2 percent thoriated tungsten rod. The internal dimensions of these will be described in the next section. The nozzles slipped into a stainless steel anode

housing which also held the injection disk and the front insulator. Graphite gaskets were placed between each component. The injection disk provided tangential propellant injection to establish swirl in the flow to stabilize the arc. The front insulator was drilled to center the cathode in the arc chamber and rectangular slots were machined along the length of its exterior to allow for propellant passage.

The rear insulator contained an inconel spring and a compression plunger. This assembly and the anode housing were held together by two stainless steel or molybdenum flanges. When mated, tolerances were such that the spring forced compression of internal seals and maximized vortex strength. Both the front and rear insulators were made from high purity boron nitride.

TEST FACILITIES

All tests involving thrust measurements were performed in vacuum Tank 8 located in the Electric Power Laboratory at the NASA Lewis Research Center. This vacuum tank is 1.5 m in diameter and 5 m long. Pumping was provided by four (30,000 LPS) oil diffusion pumps, backed by a rotary blower and two mechanical roughing pumps. Pumping speeds were such that the ambient pressure maintained was approximately 0.65 Pa (5×10^{-4} torr) at the highest propellant mass flow rate. Thrust measurements were taken using a calibrated displacement type thrust stand that has been described elsewhere in detail.[12] The entire stand was enclosed in a water-cooled copper shroud and the arcjet was mounted on a water-cooled support. This configuration effectively eliminated thermal drift. Calibration of the stand was performed both before and after each test run.

Arcjet burn-in was carried out in a vertical bell jar 0.46 m in diameter and 0.64 m in length. Pumping in the bell jar was provided by a 21,000 LPM (730 CFM) mechanical roughing pump. At the mass flow rates used in this study, the pump maintained an ambient pressure of approximately 100 Pa (0.75 torr).

In both facilities, hydrogen/nitrogen mixtures were used as the propellant. The mixture ratio was fixed at 2 to 1 to simulate fully decomposed hydrazine. The gases were supplied by standard thermal conductivity type mass flow controllers. Both mass flow rate and propellant mixture ratio must be known accurately to obtain accurate performance measurements. A calibration tank was installed in the Tank 8 flow system and in-situ flow meter calibrations were done prior to testing to insure that accurate readings were obtained.

POWER PROCESSING AND MONITORING

Pulse-width modulated power processing units designed by Gruber[10] and run with standard laboratory dc supplies were used in all tests. The design incorporated a high voltage pulse generator for arcjet starting and fast current regulation. A Hall effect current probe was used to measure the current input to the arcjet. A separate dc power supply and shunt were used to calibrate this probe before each nozzle test. The output of the probe system was fed to a digital readout and to an eight-channel strip chart recorder. Voltage measurements were taken where the power leads fed into the vacuum tank. The measurements were taken both with an isolated digital multimeter and across a 10:1 voltage divider whose output was fed to the recorder through an isolation amplifier with unity gain.

EXPERIMENTAL PROCEDURE AND OPERATING PARAMETERS

The tests were designed to investigate the effects of anode/nozzle geometry on the operating characteristics and performance of low power arcjet thrusters currently being considered for NSSK on geosynchronous communications satellites. Five different nozzle geometries were tested and are described in detail in the next section. Previous laboratory testing has shown that arcjet thrusters often require an extended burn-in period to obtain stable, steady state operation.[16] In light of this, each nozzle was put into an arcjet with a freshly ground cathode and the thruster was then installed in the bell jar for burn-in. In each case the arcjet was run until stable operation was obtained. In all cases but one, the burn-in period was at least 30 hr. The one exception was caused by power supply limitations that will be discussed in the next section.

Following burn-in, the arcjets were installed on the thrust stand for testing. As with burn-in, all thrusters except one were tested at three mass flow rates between 5×10^{-5} and 4×10^{-5} kg/sec which represents the range of flow rate typical of a satellite blowdown propellant system. The one exception was not run because of power processor limitations. Typically, arc currents between 8 and 12 A were used (in 1 A increments). The lower limit was chosen because of stability concerns while the upper limit was set by either power processor limitations or arcjet thermal considerations depending on the arcjet operating characteristics. The mass flow controllers, the current probe, and the thrust stand were calibrated before each test.

RESULTS AND DISCUSSION

ANODE/NOZZLE GEOMETRIES

The objective of this study was to examine the effects of nozzle/anode geometry on the operating characteristics of the low power dc arcjet thruster. Specifically, trends were sought to aid in future arcjet geometry optimization. To this end, five nozzles were designed and fabricated. Cross-sectional schematics of the nozzle geometries are shown in Figs. 2(a) to (e). These geometries were chosen to provide information on a wide range of design options while maintaining a reasonable test matrix and machining requirements. A detailed discussion of each is given below. Where possible, data from previous tests is also presented where it pertains to nozzle operation.

NOZZLE A

Figure 2(a) shows a cross-sectional schematic of the geometry for nozzle A which was chosen as the baseline for this study. This nozzle, as all in the set, was machined from 2 percent thoriated tungsten rod. Both the converging and diverging sections were conical with half angles of 30° and 20° respectively. The inlet diameter to the converging section was 6.4 mm in diameter to match the inner diameter of the injection disk. The constrictor was 0.64 mm in diameter and 0.26 mm in length and was the same in all nozzles to remove the effect of constrictor geometry. The area ratio (exit area:throat area) was 225.

This design was chosen as the baseline because of extensive prior experience with it in our laboratory. The nozzle inlet and outlet angles have been used extensively in other arcjet tests[6,11,12,16,17] and have produced reliable, consistent operation. Also, a number of the previously referenced studies on low Re flows have indicated that a 20° half-angle on the divergent side is a good trade-off between the friction losses taken at lesser angles and the divergence losses taken at greater angles.[14,20] While the area ratio for this nozzle is significantly greater than those judged optimal in earlier work,[15,20] unpublished work performed in our laboratory has shown that arcjet operating characteristics are influenced significantly by the location of arc attachment, and that area ratio does not strongly affect performance in the operating range of interest in this study. With the exception of the area ratio, the dimensions of the baseline nozzle are the same as those for a flight-type thruster currently under development.[15]

NOZZLE B

Nozzle B, shown in Fig. 2(b), had the same configuration on the divergent side as the baseline nozzle. To demonstrate the effect of geometry in the subsonic region, which has been shown to affect performance in gas dynamic laser nozzles (see, for example, Ref. 37), this nozzle was made with an upstream bell-shaped contour. The radius of curvature was 2.54 mm measured from the centerline as shown in the figure.

NOZZLES C AND D

Nozzles C and D are shown in Figs. 2(c) and (d) respectively. Both are identical to the baseline nozzle upstream of the constrictor exit. The downstream contours were a trumpet shape for nozzle C and a bell shape for nozzle D. An early study indicated a slight performance advantage for the trumpet nozzle in low Re flows[20] while a recent study has suggested arcjet performance in the 30 kW range may be slightly improved by a bell-shaped nozzle.[38] The bell nozzle was machined to have the same downstream contour that nozzle B had upstream and the area ratio was the same as that of nozzles A and B. The trumpet had a radius of 6.4 mm measured as shown in Fig. 2(c). The area ratio in this case is more difficult to define than in the previously described cases because the nozzle contour blends tangentially into the front face of the thruster. However, the drawing shows that is not much different than that of the baseline.

NOZZLE E

As shown in Fig. 2(e), nozzle E had bell contours both up and downstream. The contour on each side was identical, within machining tolerances, to those of nozzles B and D.

ARCJET OPERATING CHARACTERISTICS AND PERFORMANCE

Data taken from each test case are tabulated in Table I. The voltage current characteristics for the five nozzles are plotted in Fig. 3. For clarity, the figure presents only data taken at the highest mass flow rate. Similar trends were observed in both the middle and the low mass flow rate tests. Other measurements used to evaluate nozzle operating characteristics and performance are shown in Figs. 4 to 6. Figure 4 shows specific impulse versus specific power, defined as the ratio of power-to-mass flow rate. Figure 5 shows efficiency versus specific impulse and Fig. 6 gives efficiency versus specific power.

In the arcjet thruster, voltage drop occurs across three distinct regions, the cathode attachment zone (cathode fall), the arc itself, and the anode attachment zone (anode fall). Because of this, the total voltage is dependent on conditions at the cathode tip, in the nozzle, and along the constrictor and is an indicator of the arcjet operating mode. Figure 3 shows that all cases displayed typical behavior for arcjets operating in this range of power and mass flow rate. In each case the voltage decreased gradually with increasing current (at fixed mass flow rate) with no excursions that would indicate a change in operating mode. In a properly operating arcjet the anode attachment occurs in the divergent section of the nozzle. This is called high-mode operation and appeared to occur in all tests since none of the arcjets ran at the very low voltages (40 to 50 V) indicative of low mode operation; i.e., where the arc attaches in the high pressure region upstream of the constrictor.[5] Visual observation confirmed that the arc appeared to attach in the divergent section.

The data in Fig. 3 appear to fall in three distinct regions. Nozzle C (trumpet-shaped downstream) ran at significantly higher voltages than the others while nozzles A and B (conical-shaped downstream) ran at moderate voltages. The two nozzles with the bell-shaped downstream contours (D and E) ran at very low voltages compared to the others.

An evaluation of the data taken for this report and the lifetest data referenced previously[16] indicates that the observed effects can be separated and classified as: (1) upstream contour effects, (2) downstream contour effects, and (3) constrictor effects. These will be discussed in the following sections.

UPSTREAM CONTOUR EFFECTS

The effect of upstream geometry was studied by comparing results from nozzles A and B, and D and E, where the convergent section geometry differed for each pair but the constrictor and divergent section geometries were the same. Each pair consisted of one nozzle with a conical convergent contour and one with a bell-shaped convergent contour (refer to Fig. 2). These represent a very wide variation in geometry as the cone angle (in nozzles A and D) was the minimum allowed by the cathode tip and the bell contour (in nozzles B and E) had a relatively sharp corner at the constrictor entrance. The differences in operating characteristics between pairs was very large but the difference within each pair was nearly identical. In each case the nozzle with the conical contour ran about 10 V different than the nozzle with the bell-shaped contour at the same current and mass flow rate. Every attempt was made to center the cathode, hold machining tolerances, and set identical arc gaps. Duplicating geometry exactly from case to case was difficult because of the extremely small dimensions involved, and the large variance in anode geometry. Given this, it is doubtful that the differences within pairs are highly significant. The plots displayed in Fig. 4 show the performance of nozzles D and E, as measured by the specific impulse versus the specific power, to be nearly identical. The figure also shows that specific impulse from nozzle B actually was slightly below that of nozzle A at a given specific power, even though the voltage ran higher for a given current at constant mass flow rate. This difference, however, is likely not statistically significant.

The fact that the upstream contour does not have a large effect on the arcjet operating characteristics is perhaps not surprising given the geometry of the arcjet and past observations. Previous work has shown that the arc originates from a small depression in a molten pool at the cathode tip (see, for example, Refs. 11 and 16). Since the conditions at the cathode tip were similar in each test it is doubtful that the cathode fall would vary much from test to test. A magnified view of the tip region is given in Fig. 7. This shows the original cathode configurations and the erosion after in the 1000 hr lifetest recently completed.[16] As the maximum operating time on the arcjets discussed above was about 40 hr, the actual tip configuration would lie somewhere between the initial geometry and the post-test geometry of the tip used in the lifetest. Other research, to be discussed in more detail below, has shown that in arcjets with conical diverging sections, the arc attaches preferentially downstream of the constrictor exit in the low pressure region of the nozzle. This, taken with the above-mentioned observations that the arc originates from a very small spot at the cathode tip, suggests the diameter of the arc at the constrictor entrance is small compared to the constrictor diameter and so should not be grossly affected by upstream conditions.

DOWNSTREAM CONTOUR EFFECTS

Nozzles A, C, and D were used to examine the effect of downstream configuration on the arcjet operating characteristics and performance. In these nozzles, the upstream configuration and constrictor dimensions were held constant. The divergent sections were conical, trumpet-shaped, and bell-shaped, respectively. As noted previously, these nozzles ran at very different voltages (Fig. 3). Recent data from other tests have shown that, in conical arcjet nozzles, the anode attachment occurs preferentially in the low pressure region of the divergent section downstream of the constrictor exit. This research also showed that the operating voltage increases when the anode attachment zone is forced back into the higher pressure region near the constrictor exit. This indicates an increase in the anode fall voltage that more than compensates for the loss of voltage from the

shorter arc. Similar behavior was also apparent in the data taken using nozzle C. From Fig. 2(c) it can be seen that the trumpet shape has a small divergence angle following the constrictor exit before rapidly expanding. It is likely that this geometry forced the attachment immediately downstream of the constrictor, thus accounting for the higher voltage at a given current and mass flow rate. A lower current for a given power level is desirable to minimize power processor weight. Examination of performance and efficiency in Figs. 4 to 7, however, indicates that the extra power from the higher voltage at fixed current and mass flow rate is lost to the anode fall zone and goes to heating the nozzle rather than into heating the propellant. When compared to the baseline nozzle, the trumpet shape produced a specific impulse approximately 20 sec lower at a given specific power. In every case the efficiency is significantly lower at either constant specific impulse or specific power.

An opposite voltage trend was observed with the bell-shaped nozzle. This nozzle ran at a very low voltage compared to the baseline nozzle. The data suggests that the anode attachment zone, as in the case of the trumpet nozzle, also was located very close to the constrictor exit. Because of the sudden gas expansion in this region, the stream is of relatively low pressure and so the anode sheath voltage should be low. In this operating mode the arc length is less than that of the baseline nozzle. Thus, with less arc/gas interaction, both lower performance and efficiency are expected with the bell-shaped nozzle compared to the baseline nozzle. This is evident from the plots of Figs. 3 to 6. It should be noted that the low operating voltage of the bell-shaped nozzles limited the range of specific power that could be tested as the power supplies and thrusters used in this study were designed for a maximum current of 12 A. Still, the upper end of the test range for the bell-shaped nozzles did overlap the lower end of the test range obtained with the baseline nozzles, as can be seen in Fig. 4. From the figure, it is apparent that the bell-shaped contour resulted in much lower specific impulse than the baseline contour. Furthermore, the plots in Figs. 5 and 6 show that the efficiency for the nozzles with bell-shaped divergent contours, both as a function of specific impulse and specific power, was significantly lower than that obtained from any of the other nozzles tested.

CONSTRICTOR EFFECTS

A final observation is made based on information obtained in the arcjet lifetest described in Ref. 16. Tests performed to study the low Re flows in gas dynamic lasers have indicated that the radius of curvature and sharpness of the corner are important to nozzle operating characteristics.[39] Also, wind tunnel measurements have shown that wall roughness affects low Re flow.[40] These factors, however, did not seem to have much affect on the operation of the low power arcjet used in the arcjet lifetest. Figures 8 (a) to (d) show the nozzle for this arcjet before and after the 1000 hr lifetest. The nozzle was similar to nozzle A of the present study except its constrictor was 0.13 mm longer. From the figures, there was an obvious change in shape and increase in roughness in the constrictor region caused by molten tungsten. Still, measurements taken before, during, and after the test showed no significant variation in performance.

CONCLUDING REMARKS

Several nozzles were tested to study the effects of upstream and downstream contouring on arcjet thruster performance. These nozzles were tested over the range of specific power expected for NSSK on a geosynchronous communications satellite. Stable operation was obtained with all of the nozzles and both the voltage-current characteristics and visual observations indicated that the arc ran in high mode in all cases. The upstream contour had little effect on the operating characteristics and performance of the device. The same conclusion was reached regarding constrictor lip geometry and roughness from examination of past lifetest data. In contrast, the downstream geometry was found to have a substantial effect on performance. This was found to be due to the effect of downstream geometry on the location and characteristics of the arc attachment region in the anode. The rapid expansion of the bell-shaped nozzle immediately downstream of the constrictor forced this attachment into a region near the constrictor exit and led to relatively low voltage operation that yielded poor performance. The low voltage also indicated that the pressure in the attachment zone was low for the bell shape. The trumpet-shaped nozzle also forced the arc to attach near the constrictor exit. In this case, however, the high pressure near the constrictor exit forced high voltage operation. This mode of operation was less efficient than the baseline case although the performance degradation was not as severe as it was for the bell-shaped nozzle.

The baseline, conical nozzle produced the best performance. The lack of improvement over the baseline nozzle for the other geometries tested indicates that, in the near term, small changes in cone divergence angle and area ratio of the baseline conical design may best serve to optimize performance. The addition of the arc plasma to the low Re flow makes nozzle optimization in the arcjet a difficult problem. Future investigations should focus on those factors that affect the point of arc attachment in the supersonic section of the nozzle since the point of arc attachment in this region seems to have a significant effect on arcjet performance.

REFERENCES

1. McCaughey, O.J.; Geideman, W.A., Jr.; and Muller, K.: Research and Advanced Development of a 2 kW Arc-Jet Thrustor. (GRC-1646, Plasmadyne Corp.; NASA Contract NAS3-2521) NASA CR-54035, 1963.

2. Greco, R.V.; and Stoner, W.A.: Development of a Plasmajet Rocket Engine for Attitude Control. GRC-1341-A, Plasmadyne Corp., Santa Ana, CA, Dec. 1961.

3. Ducati, A.C., et al.: 1-kW Arcjet-Engine System-Performance Test. J. Spacecraft Rockets, vol. 1, no. 3, May-June 1964, pp. 327-332.

4. Wallner, L.E.; and Czika, J., Jr.: Arc-Jet Thrustor for Space Propulsion. NASA TN D-2868, 1965.

5. Curran, F.M.; and Nakanishi, S.: Low Power dc Arcjet Operation with Hydrogen/Nitrogen Propellant Mixtures. AIAA Paper 86-1505, June 1986 (NASA TM-87279).

6. Hardy, T.L.; and Curran, F.M.: Low Power dc Arcjet Operation with Hydrogen/Nitrogen/Ammonia Mixtures. AIAA Paper 87-1948, June 1987 (NASA TM-89876).

7. Knowles, S.C., et al.: Performance Characterization of a Low Power Hydrazine Arcjet. AIAA Paper 87-1057, May 1987.

8. Knowles, S.K.: Arcjet Thruster Research and Technology, Phase I. (REPT-87-R-1175, Rocket Research Co.; NASA Contract NAS3-24631) NASA CR-182107, 1987.

9. Simon, M.A., et al.: Low Power Arcjet Life Issues. AIAA Paper 87-1059, May 1987.

10. Gruber, R.P.: Power Electronics for a 1 kW Arcjet Thruster. AIAA Paper 86-1507, June 1986 (NASA TM-87340).

11. Curran, F.M.; and Haag, T.W.: Arcjet Component Conditions Through a Multistart Test. AIAA Paper 87-1060, May 1987 (NASA TM-89857).

12. Haag, T.W.; and Curran, F.M.: Arcjet Starting Reliability: A Multistart Test on Hydrogen/ Nitrogen Mixtures. AIAA Paper 87-1061, May 1987 (NASA TM-89867).

13. Sarmiento, C.J.; and Gruber, R.P.: Low Power Arcjet Thruster Pulse Ignition. AIAA Paper 87-1951, July 1987 (NASA TM-100123).

14. Knowles, S.K., et al.: Low Power Hydrazine Arcjets: A System Description for Near Term Application. 1986 JANNAF Propulsion Meeting, Vol. 1, K.L. Strange and D.S. Eggleston, eds., CPIA-PUBL-455-VOL-1, Chemical Propulsion Information Agency, Johns Hopkins University, Laurel, MD, 1986, pp. 399-408. (Avail. NTIS, AD-A178233).

15. Knowles, S.K.: Arcjet Thruster Research and Technology, Phase II. NASA CR-182276, 1989 (to be published).

16. Curran, F.M.; and Haag, T.W.: An Extended Life and Performance Test of a Low Power Arcjet. AIAA Paper 88-3106, July 1988 (NASA TM-100942).

17. Zana, L.M.: Langmuir Probe Surveys of an Arcjet Exhaust. AIAA Paper 87-1950, July 1987 (NASA TM-89924).

18. Carney, L.M.: Evaluation of the Communications Impact of a Low Power Arcjet Thruster. AIAA Paper 88-3105, July 1988 (NASA TM-100926).

19. Spisz, E.W.; Brinich, P.F.; and Jack, J.R.: Thrust Coefficients of Low Thrust Nozzles. NASA TN D-3056, 1965.

20. Murch, C.K., et al.: Performance Losses in Low-Reynolds-Number Nozzles. J. Spacecraft Rockets, vol. 5, no. 9, Sept. 1968, pp. 1090-1094.

21. Rae, W.J.: Some Numerical Results on Viscous Low-Density Nozzle Flows in the Slender-Channel Approximation. AIAA J., vol. 9, no. 5, May 1971, pp. 811-820.

22. Kallis, J.M.; Goodman, M.; and Halbach, C.R.: Viscous Effects on Biowaste Resistojet Nozzle Performance. J. Spacecraft Rockets, vol. 9, no. 12, Dec. 1972, pp. 869-875.

23. Rothe, D.E.: Electron-Beam Studies of Viscous Flow in Supersonic Nozzles. AIAA J., vol. 9, no. 5, May 1971, pp. 804-811.

24. Kuluva, N.M.; and Hosack, G.A.: Supersonic Nozzle Discharge Coefficients at Low Reynolds Numbers. AIAA J., vol. 9, no. 9, Sept. 1971, pp. 1876-1879.

25. Cline, M.C.: Computation of Two-Dimensional, Viscous Nozzle Flow. AIAA J., vol. 14, no. 3, Mar. 1976, pp. 295-296.

26. Penko, P.F.: A Numerical Technique for Analysis of Resistojet Nozzle Flow. Ph.D. Dissertation, University of Toledo, 1989.

27. Stine, H.A.; and Watson, V.R.: The Theoretical Enthalpy Distribution of Air in Steady Flow Along the Axis of a Direct-Current Electric Arc. NASA TN D-1331, 1962.

28. John, R.R.: Theoretical and Experimental Investigation of Arc Plasma-Generation Technology. ASD-TDR-62-729, Pts. I-II, Vols. 1-2, Avco Corp., Wilmington, MA, 1963.

29. John, R.R.: Thirty Kilowatt Plasmajet Rocket-Engine Development. (RAD-TR-64-6, Avco Corp.; NASA Contract NAS5-600) NASA CR-54044, 1964.

30. Watson, V.R.; and Pegot, E.B.: Numerical Calculations for the Characteristics of a Gas Flowing Axially Through a Constricted Arc. NASA TN D-4042, 1967.

31. Neuberger, A.W.: Thermo-Gasdynamical and Electrical Behavior of the Wall and Vortex-Stabilized Arc. European Space Agency, ESA-TT-220 (Translation of DLR-FB-75-38), 1975.

32. Neuberger, A.W.: Heat Transfer in Swirling Compressible Plasma Columns. AIAA Paper 75-706, May 1975.

33. Schaeffer, J.F.: Swirl Arc: A Model for Swirling, Turbulent, Radiative Arc Heater Flowfields. AIAA J., vol. 16, no. 10, Oct. 1978, pp. 1068-1075.

34. Nishida, M.; Kaita, K.; and Tanaka, K.: Numerical Studies of the Flow Field in a DC Arcjet Thruster. IEPC Conf. Paper 88-105, Nov. 1988.

35. Tanaka, K., et al.: Computational Investigation on the Characteristics of a Low Power DC Arcjet Thruster. IEPC Conf. Paper 88-106, Nov. 1988.

36. Pawlas, G.: Personal Communication, University of Toledo, Jan. 1989.

37. Greenberg, R.A., et al.: Rapid Expansion Nozzles for Gas Dynamic Lasers. AIAA J., vol. 10, no. 11, Nov. 1972, pp. 1494-1498.

38. Deininger, W.D.; Pivirotto, T.J.; and Brophy, J.R.: The Design and Operating Characteristics of an Advanced 30-kW Ammonia Arcjet Engine. AIAA Paper 87-1082, May 1987.

39. Wagner, J.L.; and Anderson, J.D., Jr.: Effect of Nozzle Throat Radius of Curvature on Gasdynamic Laser Gain. J. Spacecraft Rockets, vol. 9, no. 6, June 1972, pp. 471-473.

40. Demetriades, A.: Roughness Effects on Boundary-Layer Transition in a Nozzle Throat. AIAA J., vol. 19, no. 3, Mar. 1981, pp. 282-289.

TABLE I. - ARCJET TEST DATA

Test	Nozzle	Current	Voltage	Power, kW	m, kg/sec	Thrust, N	I_{sp}	P/m, kW/s-kg	Efficiency
1	A	0	0	0	4.07×10^{-5}	0.046	115	0	0
2	A	0	0	0	4.55	.052	116	0	0
3	A	0	0	0	4.97	.057	116	0	0
4	-	----	-----	-----	---------	-----	---	------	----
5	A	8.0	106.6	.852	4.07	.158	396	20 900	35.0
6	A	9.0	103.4	.931	4.07	.164	412	22 900	34.7
7	A	10.0	100.7	1.007	4.07	.170	425	24 700	34.3
8	A	11.0	98.6	1.084	4.07	.174	436	26 600	33.6
9	-	----	-----	-----	---------	-----	---	------	----
10	A	8.0	110.2	.882	4.55	.172	384	19 400	35.4
11	A	9.0	106.7	.960	4.55	.179	401	21 100	35.6
12	A	10.0	103.9	1.039	4.55	.186	416	22 800	35.5
13	A	11.0	102.2	1.125	4.55	.190	425	24 700	34.3
14	-	----	-----	-----	---------	-----	---	------	----
15	A	8.0	113.7	.909	4.97	.185	380	18 300	36.7
16	A	9.0	109.4	.984	4.97	.191	392	19 800	36.2
17	A	10.0	107.2	1.072	4.97	.199	408	21 600	36.0
18	A	11.0	105.2	1.158	4.97	.206	422	23 300	35.8
19	-	----	-----	-----	---------	-----	---	------	----
20	-	----	-----	-----	---------	-----	---	------	----
21	B	0	0	0	4.07	.044	109	0	0
22	B	0	0	0	4.55	.049	109	0	0
23	B	0	0	0	4.97	.053	108	0	0
24	-	----	-----	-----	---------	-----	---	------	----
25	B	8.0	117.6	.941	4.07	.158	395	23 110	31.6
26	B	9.0	113.6	1.022	4.07	.163	408	25 110	31.2
27	B	10.0	111.2	1.112	4.07	.169	423	27 310	30.9
28	B	11.0	108.9	1.198	4.07	.174	437	29 420	30.6
29	B	12.0	107.6	1.291	4.07	.179	449	31 710	30.1
30	-	----	-----	-----	---------	-----	---	------	----
31	B	8.0	122.0	.976	4.55	.175	391	21 470	33.4
32	B	9.0	117.7	1.059	4.55	.181	406	23 290	33.2
33	B	10.0	115.1	1.151	4.55	.187	420	25 310	32.8
34	B	11.0	113.0	1.243	4.55	.193	434	27 340	32.4
35	B	12.0	111.6	1.339	4.55	.199	446	29 440	31.8
36	-	----	-----	-----	---------	-----	---	------	----
37	B	8.0	124.4	.995	4.97	.184	378	20 010	33.4
38	B	9.0	120.6	1.085	4.97	.191	392	21 820	33.0
39	B	10.0	117.7	1.177	4.97	.198	406	23 660	32.8
40	B	11.0	116.0	1.276	4.97	.205	421	25 650	32.5
41	B	12.0	114.6	1.375	4.97	.212	435	27 640	32.2
42	-	----	-----	-----	---------	-----	---	------	----
43	-	----	-----	-----	---------	-----	---	------	----
44	C	0	0	0	4.07	.044	111	0	0
45	C	0	0	0	4.55	.049	111	0	0
46	C	0	0	0	4.97	.054	111	0	0
47	-	----	-----	-----	---------	-----	---	------	----
48	C	11.0	128.0	1.408	4.07	.190	476	34 594	30.9
49	-	----	-----	-----	---------	-----	---	------	----
50	C	8.1	139.0	1.120	4.55	.180	407	24 786	31.6
51	C	9.1	135.0	1.223	4.55	.187	423	27 060	31.3
52	C	10.1	132.0	1.333	4.55	.196	442	29 496	31.4
53	C	11.1	131.0	1.441	4.55	.203	458	31 880	31.2
54	-	----	-----	-----	---------	-----	---	------	----
55	C	8.1	141.0	1.139	4.97	.193	397	22 918	32.2
56	C	9.1	138.0	1.261	4.97	.202	414	25 372	31.7
57	C	10.1	135.0	1.364	4.97	.210	430	27 445	31.7
58	C	11.1	133.0	1.463	4.97	.217	444	29 437	31.5
59	-	----	-----	-----	---------	-----	---	------	----
60	-	----	-----	-----	---------	-----	---	------	----
61	D	0	0	0	4.07	.041	102	0	0
62	D	0	0	0	4.55	.046	102	0	0
63	D	0	0	0	4.97	.050	102	0	0
64	-	----	-----	-----	---------	-----	---	------	----
65	D	8.0	84.7	.678	4.07	.125	314	16 650	27.6

TABLE I. - Concluded.

Test	Nozzle	Current	Voltage	Power, kW	m, kg/sec	Thrust, N	I_{sp}	P/m, kW/s-kg	Efficiency
66	D	9.0	81.9	0.737	4.07	0.129	322	18 110	26.9
67	D	10.0	80.7	.807	4.07	.134	335	19 830	26.5
68	D	11.0	79.5	.874	4.07	.138	345	21 470	26.1
69	D	12.0	77.9	.935	4.07	.141	353	22 950	25.7
70	-	----	-----	-----	---------	-----	---	------	----
71	D	8.0	85.9	.687	4.55	.137	307	15 110	29.0
72	D	9.0	83.5	.752	4.55	.142	318	16 530	28.6
73	D	10.0	82.1	.821	4.55	.147	329	18 050	28.1
74	D	11.0	80.9	.890	4.55	.151	339	19 560	27.5
75	D	12.0	79.9	.959	4.55	.156	350	21 090	27.3
76	-	----	-----	-----	---------	-----	---	------	----
77	D	8.0	87.1	.697	4.97	.149	305	14 010	30.8
78	D	9.0	84.7	.762	4.97	.153	314	15 320	30.0
79	D	10.0	83.3	.833	4.97	.159	325	16 750	29.5
80	D	11.0	82.6	.909	4.97	.164	336	18 260	28.8
81	D	12.0	81.9	.983	4.97	.168	345	19 760	28.3
82	-	----	-----	-----	---------	-----	---	------	----
83	-	----	-----	-----	---------	-----	---	------	----
84	-	----	-----	-----	---------	-----	---	------	----
85	-	----	-----	-----	---------	-----	---	------	----
86	-	----	-----	-----	---------	-----	---	------	----
87	E	0	0	0	4.07	.040	100	0	0
88	E	0	0	0	4.55	.045	101	0	0
89	E	0	0	0	4.97	.049	101	0	0
90	-	----	-----	-----	---------	-----	---	------	----
91	E	8.0	71.9	.575	4.07	.121	304	14 130	30.3
92	E	9.0	69.4	.625	4.07	.124	311	15 330	29.4
93	E	10.0	67.7	.677	4.07	.128	320	16 630	28.8
94	E	11.0	66.6	.733	4.07	.132	330	17 990	28.3
95	E	12.0	65.8	.790	4.07	.135	390	19 410	27.8
96	-	----	-----	-----	---------	-----	---	------	----
97	E	8.0	74.5	.596	4.55	.132	296	13 100	31.1
98	E	9.0	72.1	.649	4.55	.135	302	14 270	29.8
99	E	10.0	70.2	.702	4.55	.141	316	15 450	30.1
100	E	11.0	68.9	.758	4.55	.145	325	16 670	29.5
101	E	12.0	68.2	.818	4.55	.149	334	17 980	29.1
102	-	----	-----	-----	---------	-----	---	------	----
103	E	8.0	75.5	.604	4.97	.140	288	12 140	31.5
104	E	9.0	73.1	.658	4.97	.145	296	13 230	30.8
105	E	10.0	71.7	.717	4.97	.150	307	14 410	30.5
106	E	11.0	70.5	.776	4.97	.155	317	15 590	30.0
107	E	12.0	69.9	.839	4.97	.160	327	16 860	29.7

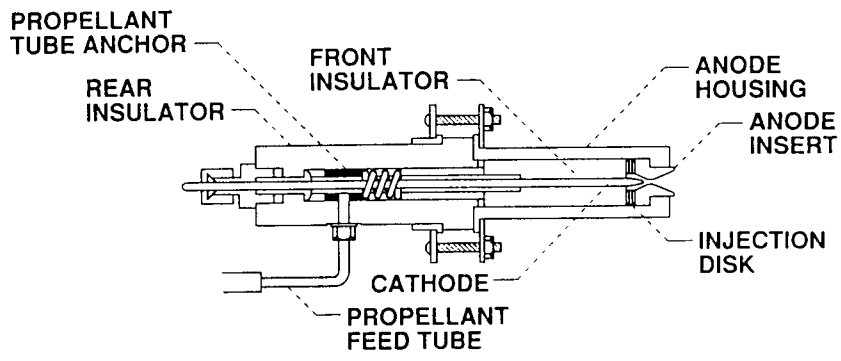

Figure 1. - Cutaway view of arcjet thruster.

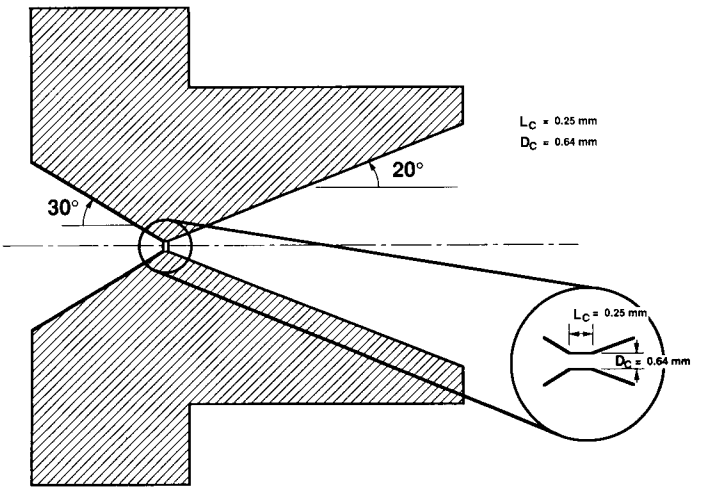

(a) Baseline conical nozzle.

Figure 2. - Nozzle configurations.

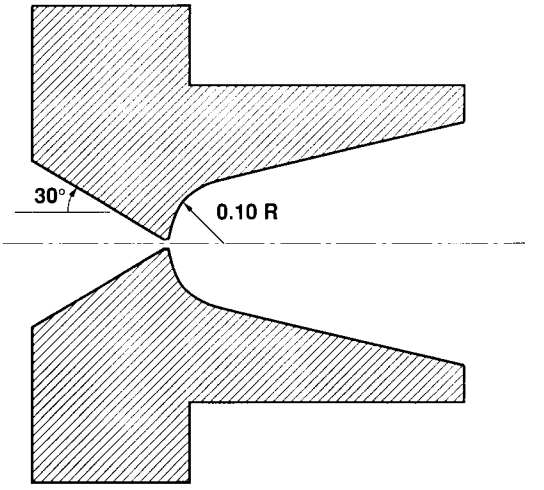

(d) Downstream bell-shaped nozzle.

Figure 2. - Continued.

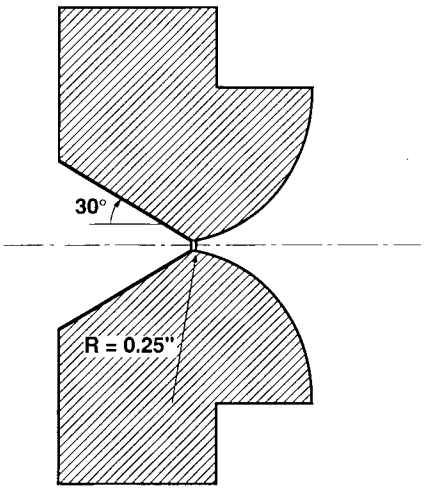

(c) Downstream trumpet-shaped nozzle.

Figure 2. - Continued.

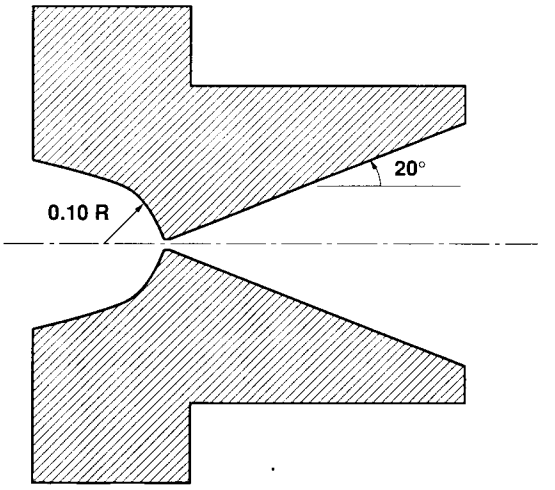

(b) Upstream bell-shaped nozzle.

Figure 2. - Continued.

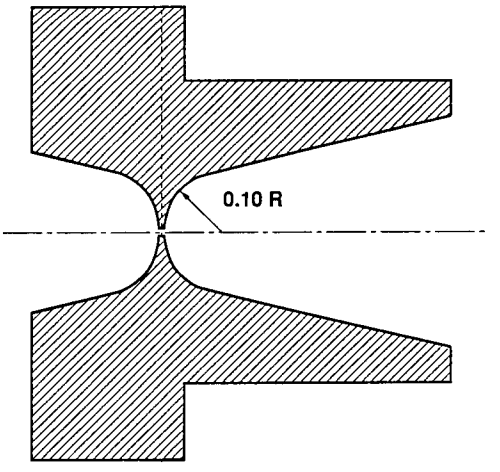

(e) Upstream/Downstream bell-shaped nozzle.

Figure 2. - Concluded.

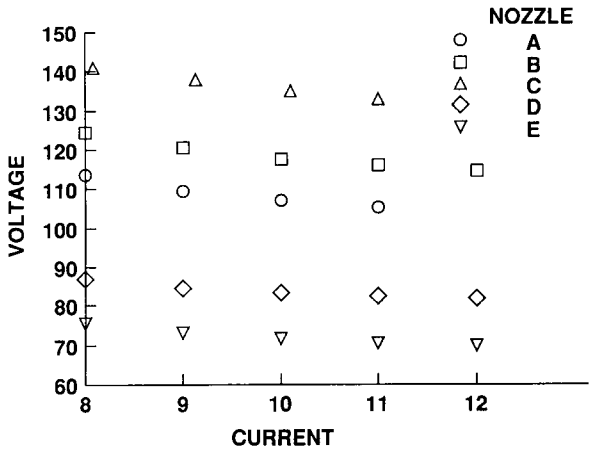

Figure 3. - Current - voltage characteristics ($\dot{m}$ = 4.97e-5 kg/sec).

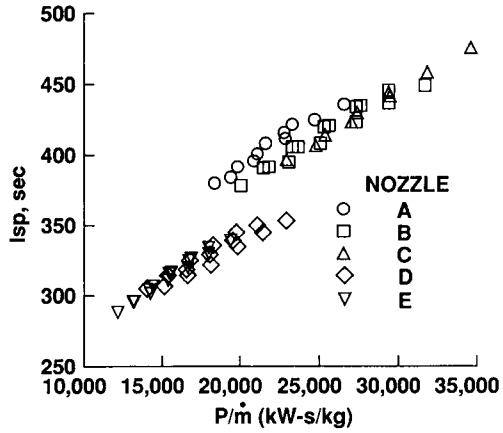

Figure 4. - Isp versus specific power.

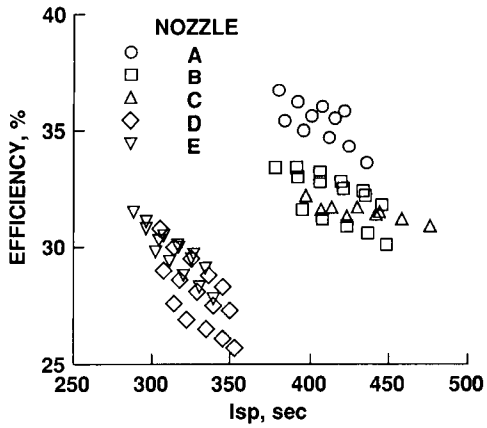

Figure 5. - Efficiency versus Isp.

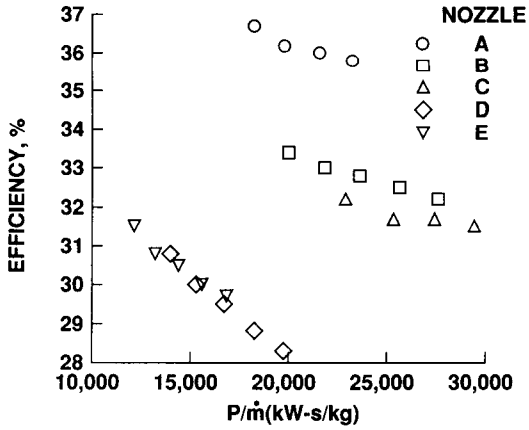

Figure 6. - Efficiency versus specific power.

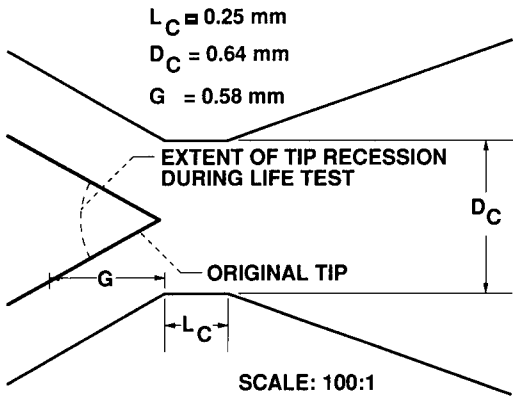

Figure 7. - Electrode position in baseline nozzle configuration.

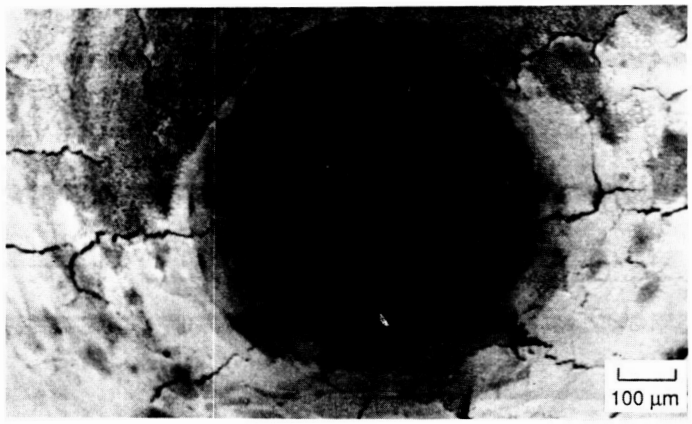

(b) SEM of convergent side of anode (post test).

(c) SEM of constrictor (post test).

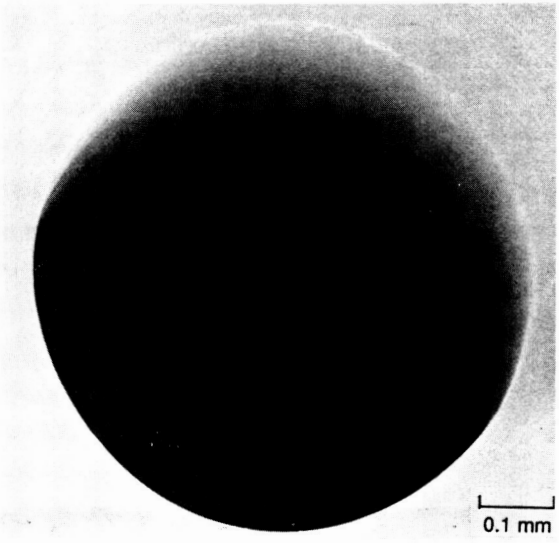

(a) Photomicrograph of converging side of anode (pretest).
Note: divergent side similar.

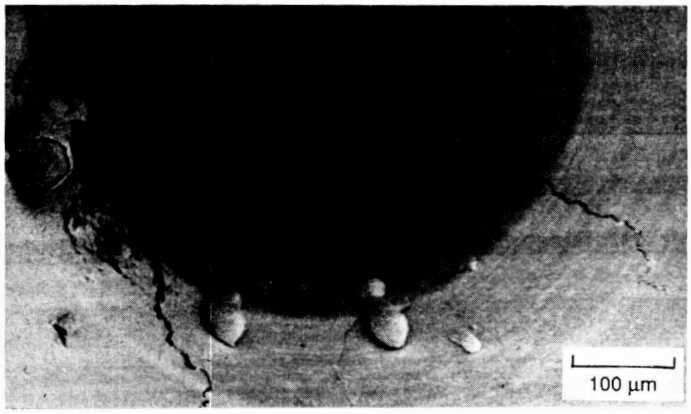

(d) SEM of divergent side of anode (post test).

Figure 8. - Pre- and post test anode conditions of 1000 hr life-test anode. (Taken from reference 16).

NASA
National Aeronautics and Space Administration

Report Documentation Page

1. Report No.	2. Government Accession No.	3. Recipient's Catalog No.
NASA TM-102050		

4. Title and Subtitle	5. Report Date
Arcjet Nozzle Design Impacts	
	6. Performing Organization Code

7. Author(s)	8. Performing Organization Report No.
Francis M. Curran, Amy J. Sovie, and Thomas W. Haag	E-4802
	10. Work Unit No. 506-42-32

9. Performing Organization Name and Address	11. Contract or Grant No.
National Aeronautics and Space Administration Lewis Research Center Cleveland, Ohio 44135-3191	
	13. Type of Report and Period Covered Technical Memorandum

12. Sponsoring Agency Name and Address	14. Sponsoring Agency Code
National Aeronautics and Space Administration Washington, D.C. 20546-0001	

15. Supplementary Notes

Prepared for the 1989 JANNAF Propulsion Meeting, Cleveland, Ohio, May 23-25, 1989. Francis M. Curran and Thomas W. Haag, NASA Lewis Research Center; Amy J. Sovie, Ohio University, Electrical Engineering Dept., Athens, Ohio 45701 and Summer Student Intern at NASA Lewis Research Center.

16. Abstract

An experimental investigation was conducted to determine the effect of nozzle configuration on the operating characteristics of a low power dc arcjet thruster. A conical nozzle with a 30° converging angle, a 20° diverging angle, and an area ratio of 225 served as the baseline case for the study. Variations on the geometry included bell-shaped contours both up and downstream, and a downstream trumpet-shaped contour. The nozzles were operated over a range of specific power near that anticipated for on-orbit operation. Mass flow rate, thrust, current, and voltage were monitored to provide accurate comparisons between nozzles. The upstream contour was found to have minimal effect on arcjet operation. It was determined that the contour of the divergent section of the nozzle, that serves as the anode, was very important in determining the location of arc attachment, and thus had a significant impact on arcjet performance. The conical nozzle was judged to have the optimal current/voltage characteristics and produced the best performance of the nozzles tested.

17. Key Words (Suggested by Author(s))	18. Distribution Statement
Electric propulsion Arcjet thruster Nozzle design	Unclassified – Unlimited Subject Category 20

19. Security Classif. (of this report)	20. Security Classif. (of this page)	21. No of pages	22. Price*
Unclassified	Unclassified	14	A03

NASA FORM 1626 OCT 86

*For sale by the National Technical Information Service, Springfield, Virginia 22161